Agricultural Water Management 302 (2024) 109007

Contents lists available at ScienceDirect

Agricultural Water Management

journal homepage: www.elsevier.com/locate/agwat

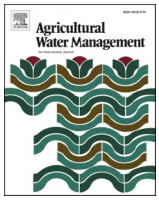

Optimal groundwater depth and irrigation amount can mitigate secondary salinization in water-saving irrigated areas in arid regions

Wenhao Li [a,b,c], Shaozhong Kang [a,b,c,*], Taisheng Du [a,b,c], Risheng Ding [a,b,c], Minzhong Zou [a,b,c]

[a] Center for Agricultural Water Research in China, China Agricultural University, Beijing 10083, China
[b] State Key Laboratory of Efficient Utilization of Agricultural Water Resources, Beijing 10083, China
[c] National Field Scientific Observation and Research Station on Efficient Water Use of Oasis Agriculture, Wuwei, Gansu 733009, China

ARTICLE INFO

Handlin g Editor: Dr Z. Xiying.

Keywords:
Water saving irrigation district
Soil salinity
Spatiotemporal variability
Influencing factor
Regulation scheme

ABSTRACT

Secondary salinization poses a significant threat to the sustainable development of water-saving irrigation districts. This study aims to explore the spatial and temporal variations in soil salinity and the factors influencing these changes in water-saving irrigation areas in the inland arid regions of Northwest China. The Manas River Irrigation District was selected as the study area. A grid measuring 10 km × 14 km grid was designed to determine the latitude and longitude coordinates of the grid centers, resulting in 66 sample points. Soil samples were collected from these points in 2013, 2014, 2020, and 2021 from the 0—100 cm layer to obtain salinity data. Based on existing research and practical conditions in water-saving irrigation areas, 11 factors influencing soil salinity changes were identified, including irrigation area and irrigation amount. Classical statistical methods and interpretable machine learning techniques were employed to analyze the distribution characteristics of soil salinity and the influencing factors. This analysis proposes effective solutions to mitigate potential secondary salinization in irrigation areas. The results revealed that soil salinity in the irrigation area belonged to moderate variation (C_v = 46.74 %—51.80 %). The horizontal direction of the irrigation area shows higher salt content in the upstream and downstream areas, and a gradual decrease in variability with increasing depth characterizes the vertical direction. From 2013–2021, soil salinization in the irrigation area gradually decreased. In 2013 and 2014, the area was predominantly covered by mild saline-alkali soil, accounting for 75.1 % and 76.6 % of the total area, respectively. However, in 2020 and 2021, non-saline soils became dominant, covering 60.9 % and 66.5 % of the total irrigation area, respectively. In order of importance, the factors affecting the spatial and temporal evolution of soil salinity are groundwater depth, annual water surface evaporation, water-saving irrigation area, underground water diversion amount, mineralization of groundwater, irrigation amount, surface water diversion amount, and annual rainfall. In the oasis irrigation area, maintaining a groundwater depth of 4.0—6.0 m and an irrigation amount of 5500—6000 m^3 ha^{-1} can alleviate the problem of secondary salinization that may result from large-scale development of water-saving irrigation. The findings of this study provide a basis for the prevention and control of soil salinization in water-saving irrigation areas and the development and management of saline land in oasis areas.

1. Introduction

Northwest China has a temperate continental climate with typical characteristics of semi-arid or arid. Xinjiang is located in the central Eurasian continent, located in the northwest border, with a total land area of 166.49×10^4 ha, accounting for about 1/6 of the country. The total amount of water resources is 8.35×10^{10} m^3, which is only 3 % of the national total, and the shortage of water resources has become an important factor restricting the region's development (Shen et al., 2013). Xinjiang is rich in agricultural resources and is a significant agricultural production and supply base and grain production reserve base in China. Regional irrigation water consumption has consistently accounted for more than 90 % of the total water consumption in the region (Li et al., 2015). Drip irrigation technology has the characteristics of high-frequency irrigation, avoiding deep leakage and effectively improving water use efficiency (Danierhan et al., 2013). In 1996, drip irrigation technology began to be applied in the Manas River irrigation area. It has shown significant water-saving and yield-increasing effects

* Corresponding author at: Center for Agricultural Water Research in China, China Agricultural University, Beijing 10083, China.
E-mail address: kangsz@cau.edu.cn (S. Kang).

https://doi.org/10.1016/j.agwat.2024.109007
Received 20 June 2024; Received in revised form 8 August 2024; Accepted 9 August 2024
Available online 16 August 2024
0378-3774/© 2024 The Authors. Published by Elsevier B.V. This is an open access article under the CC BY-NC-ND license (http://creativecommons.org/licenses/by-nc-nd/4.0/).

in production and has been rapidly promoted in arid areas, becoming China's most important water-saving irrigation technology (Deng et al., 2006). However, the widespread application of drip irrigation has altered water and salt transport and groundwater recharge processes. This has led to a new spatial distribution pattern of soil salinity, which may create water-saving irrigation-based secondary salinization problems in the irrigation areas(Hopmans et al., 2021; Karimzadeh et al., 2024).

Excessive soil salt content will lead to decreased fertility and seriously affect the expected growth of crops (Salcedo et al., 2022). It has become essential in restricting agricultural development (Haj-Amor et al., 2022; Li et al., 2022). Many experts and scholars have explored the spatial variability of soil salinity from the perspectives of different scales, watersheds, and environmental conditions. Sun et al. (2022) studied the spatial and temporal dynamics of soil salinity in arid agricultural areas and found that soil salinity has a robust spatial dependence. The spatial variability of soil salinity in the Adakan region of central Iran, the Erbil Lake region of Xinjiang, and the Hetao Irrigation District was characterized by geostatistical methods by previous authors (Taghizadeh-Mehrjardi et al., 2014; Ren et al., 2019; Wang et al., 2019a). Scudiero et al. (2014) used Landsat 7 surface reflectance data to retrieve soil salt content and analyzed the spatial distribution of soil salt in California. The soil salt content is different in different spatial positions at the same time, and significantly different at different times in the same spatial position (Yao and Yang, 2010). The above studies focus on spatial variation of soil salinity to provide a basis for guiding regional agricultural development and provide methods for researchers working on the spatial and temporal evolution of soil salinity in water-saving irrigation areas.

Soil properties are influenced by a combination of human activities, climate, parent material, and topography (Feng et al., 2022). Salt moves with water, and any factor that affects soil water movement will result in changes in soil salinity (Corwin, 2021). Zhao et al. (2023) showed that the main factors affecting soil salinity in cropland during the crop reproductive period were irrigation, precipitation, and crop cultivation, and the main factors affecting soil salinity in wasteland were precipitation and topography. Taghizadeh-Mehrjardi et al. (2014) concluded that soil salinization was mainly affected by irrigation methods, water quality, and water quantity. Xie et al. (2021) believed that the salt content of shallow and deep groundwater affected the spatial distribution characteristics of soil salinity. Wei et al. (2020) investigated the spatial variability of soil salinity at the watershed scale in a northwestern oasis and found that geographic elevation was a critical factor in the spatial variability of soil salinity. In drip-irrigated farmland, irrigation can significantly change the soil salinity distribution in the crop root zone, with the coefficient of variation (C_v) of soil salinity increasing from 45.2 % to 64.5 % after irrigation (Hammad et al., 2023).With the increase in irrigation amount and soil depth, the variability of soil salinity in the root zone decreased (Hou et al., 2022). So, how does soil salinity evolve spatially and temporally in water-saving irrigation areas where drip irrigation under membranes is promoted on a large scale in production practice, and what factors influence salinity changes?

The objectives of this study were threefold: (1) to investigate the spatial distribution of soil salinity and its variations in a large area of drip irrigation under a membrane, (2) to identify the factors influencing the distribution of salinity in water-saving irrigation areas and their contribution, (3) to determine a regulation scheme for the sustainable development of irrigation areas to analyze soil salinity's spatial and temporal evolution. This analysis fills the gaps in the water-saving irrigation area in arid area and provides a scientific basis for preventing and controlling soil salinization and ensuring sustainable development in irrigation areas.

2. Materials and methods

2.1. Overview of the experimental area

The Manas River Irrigation District (now referred to as the "Irrigation District") (84°42'～86°32'E, 44°10'～45°22'N) is located in the core of the economic belt on the northern slopes of the Tianshan Mountains in Xinjiang, China, in the hinterland of the Asian-European continent (Fig. 1). It is located at the southern edge of the Junggar Basin, with a typical inland arid climate, covering an area of about 1.1×10^4 km^2, the largest oasis area in Xinjiang, and the fourth largest irrigation area in China. The irrigation district's minimum temperature is −42.8 °C, and the highest is 43.1 °C. The annual average temperature for is 6.5 °C; the annual frost-free period of 148–187 d, 2745 h sunshine hours. The climatic conditions here are suitable for crop growth and are an important high-quality cotton production base in China. The average annual rainfall is 125.0–207.7 mm, and the average annual evaporation is 1500–2100 mm, China's most typical desert oasis irrigation agricultural area. The Manas River irrigation district is mainly irrigated by runoff and groundwater from inland rivers such as the Manas River. This model of water resources development and utilization is more common in arid irrigation areas in Northwest China. However, the proportion of agricultural water in the irrigation area continues to be too high, accounting for about 91.70 % of the total water diversion in the past 30 years. Drip irrigation under film began to be popularized and applied in the irrigation area in 1996 and has become the most important water-saving irrigation technology in this area. In 2013, the irrigation district of the irrigation area was 6.80×10^6 ha, and the area of drip irrigation under film was 5.71×10^6 ha. accounting for 83.97 %; In 2021, the irrigation district of the irrigation area was 8.44×10^6 ha, of which the area of drip irrigation under film is 7.75×10^6 ha, accounting for 91.82 %. Compared with 2013, the water-saving irrigation area increased by 2.04×10^6 ha in 2021, accounting for 7.85 %.

2.2. Sample collection and processing

The Manas River Irrigation District base map (vector boundary map), which cooperates with the irrigation district's water management department, was used to lay out long-term observation wells for ground level and groundwater mineralization. ArcGIS 10.8 (https://www.esri.com/zh-cn/home) was used to design a 10 km×14 km grid, totaling 66 (Fig. 2). The selected centroid points have the following points: Centroid points should be located in the farmland area to ensure that the sample can represent the farmland characteristics in the grid ; The selection of grid centroid takes into account the uniform distribution of farmland and avoids the deviation of sampling results ; The selection of the centroid position ensures the availability and accessibility of farmland data, which includes actual geographic data and access rights. Derive the grid center of mass latitude and longitude coordinates to determine the location of the sampling points. Soil samples from agricultural fields near the grid's center of mass were collected at the beginning of April (before sowing on agricultural fields) and at the end of October (after harvesting the crops) in 2013, 2014, 2020, and 2021, respectively. These years represent different climatic stages or trends, especially the changes of key climatic factors such as precipitation and evaporation, which have an important impact on the distribution and dynamics of soil salinity. The layers were obtained according to 0—20 cm, 20—40 cm, 40—60 cm, 60—80 cm, 80—100 cm and filled in aluminum boxes. The samples were brought back to the laboratory to be naturally air-dried, ground, and sieved to remove impurities. The fitting equation of conductivity and soil salt content was obtained by conductivity method and dry residue method. The conductivity of the extract was measured by a conductivity meter (DDS-11A digital display, Shanghai Leici). The formula for calculating the salt content is as follows:

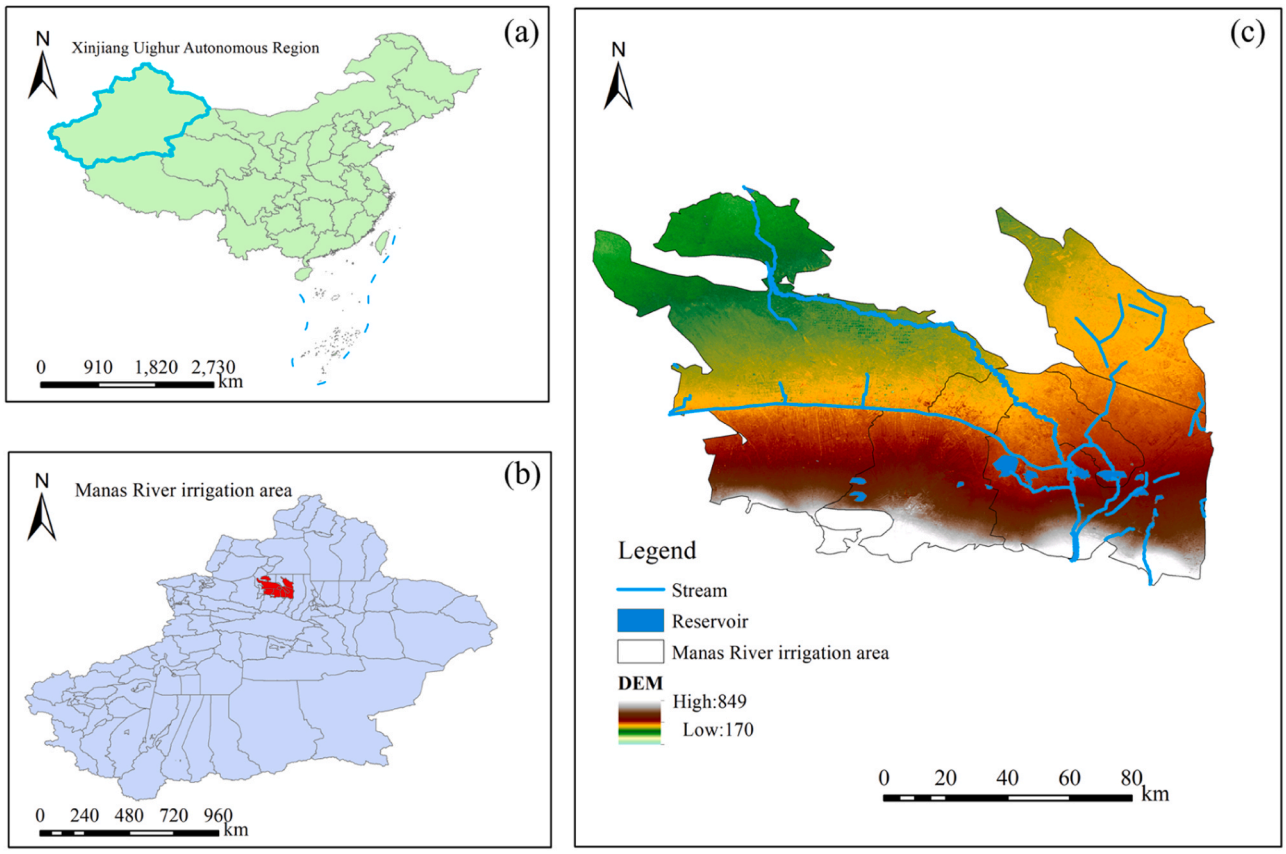

Fig. 1. The geographical location of the Manas River Irrigation Area in China (a) and Xinjiang (b), as well as the distribution status in the Manas River Basin (c).

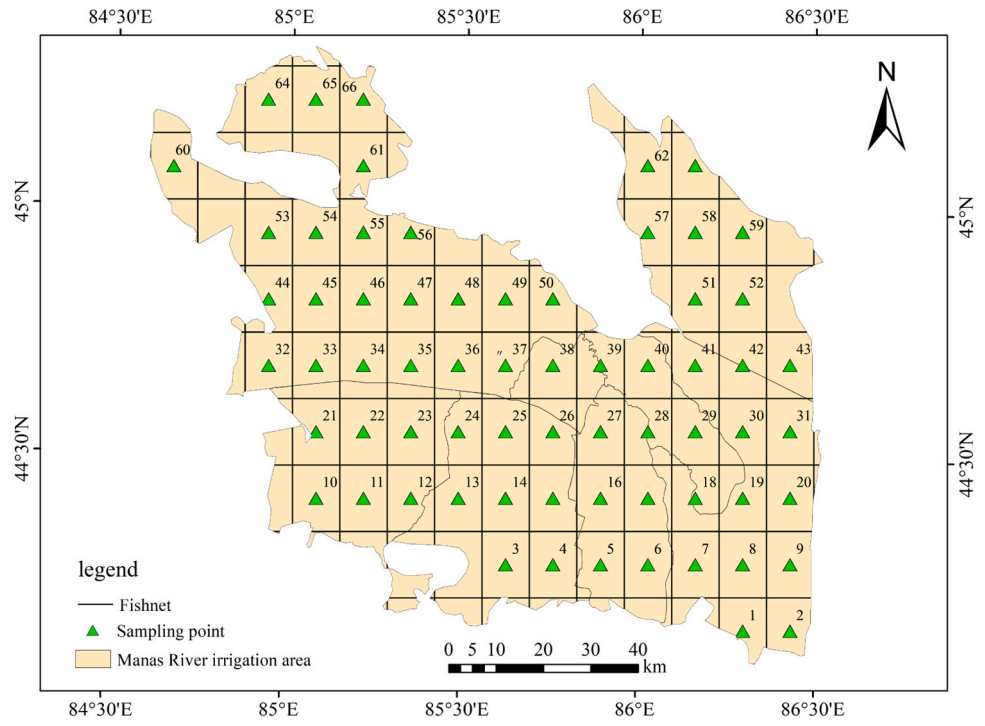

Fig. 2. Sampling point grid and sample distribution map in the study area.

$$y = 0.0004x - 0.0341, R^2 = 0.9905 \quad (1)$$

In the formula: y is the salt content ($g \cdot kg^{-1}$); x is the conductivity ($\mu S \cdot cm^{-1}$). The mean value of the two sample data in the same year was determined as the annual salt data.

Organize annual irrigation reports for 2013, 2014, 2020, and 2021

for Shihezi City, Shawan City, and Manas County. Obtain data on the irrigated area (IA), water-saving irrigation area (WSIA), underground water diversion amount (UWDA), and surface water diversion amount (SWDA) for each township and mission in the Manas River Irrigation District. Kriging interpolation was performed on the data using ArcGIS 10.8 to extract the data corresponding to the 66 grids. Further, calculate the irrigation amount of each grid = (surface water diversion amount + underground water diversion amount) / irrigation area. Groundwater depth and mineralization of groundwater data were obtained from 66 long-term observation wells in three counties and cities. Annual rainfall and annual water surface evaporation were obtained from nine meteorological stations of the meteorological bureaus of three counties and cities and the water-saving irrigation experimental station of Shihezi University. Similarly, ArcGIS 10.8 is used to interpolate the data and extract the data corresponding to 66 grids. Sampling point elevation data were obtained using a GARMIN (https://www.garmin.com.cn/) handheld GPS during sampling in 2013. The ring knife method was used to test the 0—20 cm soil bulk weight at each sampling. In agricultural production, 0—20 cm soil layer is usually considered to be the main tillage layer, which is the most densely distributed area of crop roots. The soil properties of this soil layer have a direct impact on the growth and development of crops (Mut et al., 2022).

2.3. Research methods

2.3.1. Classical statistical methods

The classical statistical method assumes that the variables are purely random and that the samples are independent and obey a known probability distribution. In the vertical direction, the soil is divided into five uniform soil layers, and the Irrigation district is divided into 66 uniform regions in the plane. The spatial variation of soil salinity was described by calculating the mean, standard deviation, variance, maximum, minimum, coefficient of variation, and significance test. The dispersion degree of salt in different soil layers and grids is reflected by the coefficient of variation (C_V). C_V <10 % is considered weak variance, 10 %≤ C_V≤ 100 % is considered moderate variance, and C_V> 100 % is considered substantial variance (Rosemary et al., 2017).

2.3.2. Random Forest (RF) salt model and SHAP algorithm

RF is a machine learning model consisting of multiple decision trees integrated to train and test samples, developed from traditional classification and regression trees. It has higher prediction accuracy and better generalization performance than a single decision tree. Therefore, it has the advantages of high efficiency and avoiding over-fitting when simulating and predicting salt changes (John et al., 2022). This study used the random forest method to construct the salt model. The coefficient of determination (R^2), mean absolute error (*MAE*), and root mean square error (*RMSE*) were used to characterize the model's interpretation of soil salinity. The formula is as follows:

$$R^2 = 1 - \frac{\sum_{i=1}^{n}(x_i - y_i)^2}{\sum_{i=1}^{n}(x_i - \overline{X})^2} \tag{2}$$

$$MAE = \frac{1}{n}\sum_{i=1}^{n}|x_i - y_i| \tag{3}$$

$$RMSE = \sqrt{\frac{1}{n}\sum_{i=1}^{n}(x_i - y_i)^2} \tag{4}$$

where x_i denotes the measured value; y_i denotes the predicted value; $\overline{x}$denotes the mean value of the measured value; and n denotes the number of measured samples.

The Shapley Additive Explanations (SHAP) algorithm constructs an additive interpretation model inspired by the Shapley value. It can provide a SHAP value for each feature, indicating the contribution of the feature to model prediction. By setting the threshold of the SHAP value, the features that have an important influence on the model prediction results can be screened out. In the calculation process, the Shapley value is used to reflect the contribution of features to the model's prediction ability, and the specific expression of the nonlinear mapping is further optimized. The model produces a prediction value for each prediction sample, and the output SHAP value is the value assigned to each feature in the sample (Meng et al., 2020). Therefore, in analyzing the factors influencing spatial and temporal changes in soil salinity in the irrigation district, the SHAP value directly reflects the importance of these factors in the spatial and temporal distribution of salinity. The higher the SHAP value of a feature, the more significant the impact on soil salinity in the irrigation district. The positive and negative SHAP values can also reflect the positive or negative relationship between the influencing factors and soil salinity. The calculation formula is as follows:

$$\phi_j\left(val\right) = \sum_{s\subseteq\left\{x_{1,\ldots,x_p}\right\}/\left\{x_j\right\}} \frac{|s|!(p-|s|-1)!}{P!}\left(val\left(s\cup\left\{x_j\right\}\right) - val(s)\right) \tag{5}$$

where $\phi_j(val)$ is the Shapley value of feature j, representing the contribution to the result; s is a subset of features used in the model; x is the vector to explain the sample eigenvalues; p is the number of features; $\frac{|s|!(p-|s|-1)!}{P!}$ represents the weight; $val(s)$ is the output value under feature s.

$$g = \varnothing_0 + \sum_{i=1}^{M}\varnothing_j \tag{6}$$

where g is an explanatory model; m is the number of input features; ϕ_j is the Shapley value of feature j; ϕ_0 is the predicted mean of all samples.

2.4. Data analysis

Experimental data were analyzed using SPSS 26.0 (IBM, Inc., Armonk, NY, USA) for descriptive statistics, Kolmogorov-Smirnov (K-S) test, Pearson correlation analysis, and analysis of covariance. Trend analysis, extraction of relevant information, and editing and output of salt distribution graphs were performed using ArcGIS 10.8, and some data processing and graphs were performed using Origin 2021 (Origin Lab, Northampton, MA, USA).

3. Results and discussion

3.1. Spatial distribution and variation of soil salinity in oasis water-saving irrigation district

3.1.1. Descriptive statistics

Table 1 shows the descriptive statistics and K-S normality test of salt in different soil layers in the irrigation district. In 2013, 2014, 2020, and 2021, the variation coefficient C_v of soil salinity in the Manas River irrigation area's 0—100 cm soil layer ranged from 46.74 % to 51.80 %, which belonged to moderate variation. The maximum value, minimum value, average value, standard deviation, and coefficient of variation of salt all showed an overall decreasing trend with the increase of soil depth. The soil salinity in the irrigation district showed the distribution characteristics of surface accumulation in the vertical direction. The average salt content of the surface soil in the irrigation district in four years was 3.17 g kg^{-1}, which gradually decreased to 2.68 g kg^{-1} in 100 cm. Among them was a small salt accumulation in the 60 cm soil layer, with a salt content of 2.80 g kg^{-1}. The KS significance was greater than 0.05, indicating that the soil salt content in each soil layer obeyed the normal distribution under the 95 % confidence interval.

3.1.2. Spatial distribution patterns

The years 2013, 2014, 2020, and 2021 are characterized by a higher salt content distribution in the upstream and downstream areas of the

Table 1
Descriptive statistics and K-S test of soil salinity.

Soil depths (cm)	Max (g kg^{-1})	Min (g kg^{-1})	Mean (g kg^{-1})	Vr	C_v (%)	Skew	Kurt	P-KS
0	6.97	0.32	3.17	1.48	46.74	0.50	0.46	0.056*
20	6.22	0.35	2.66	1.34	50.28	0.65	0.14	0.076*
40	6.36	0.25	2.74	1.35	49.42	0.63	0.13	0.065*
60	6.48	0.33	2.80	1.40	49.90	0.60	0.29	0.076*
80	6.30	0.23	2.66	1.38	51.80	0.63	0.24	0.072*
100	6.46	0.22	2.68	1.37	51.23	0.66	0.18	0.061*

Note: * represents a significant level of 10 %.

irrigation district (Fig. 3). In 2013 and 2014, the soil salt content in the high salt area was about 5.5—6.0 g kg^{-1}. In 2020 and 2021, the soil salt content in the low-salt area was about 1.0—1.5 g kg^{-1}. In 2013, the soil salt in the southeast of the irrigation area was 4–6 g·kg^{-1}. In 2014, the soil salinity in the southeast of the irrigation area was 4–5.5 g·kg^{-1}. In 2020, the soil salt in the southeast of the irrigation area was 2.5–3.5 g·kg^{-1}. In 2021, the soil salt in the southeast of the irrigation area was 2–3.5 g·kg^{-1}. Over time, soil salinity in the 0—100 cm soil layer of the irrigation district showed a decreasing trend year by year. Classification criteria according to soil salinization (Bouksila et al., 2013), in 2013 and 2014, the irrigation district was dominated by mild saline-alkali soil, accounting for 75.1 % and 76.6 % of the total area, respectively. The irrigation district was dominated by non-saline soils in 2020 and 2021, accounting for 60.9 % and 66.5 % of the total irrigation district, respectively. Wang et al. (2019b) and Li et al. (2023) studied the variation characteristics of soil salinity in cotton fields with long-term continuous drip irrigation in an oasis area by using the spatial-temporal variation method and fixed-point monitoring method, respectively. The results showed that the soil salinity decreased from year to year with the increase of drip irrigation years. The study of Zong et al. (2023) found that the application of drip irrigation under a membrane in an oasis irrigation area was a rapid desalination stage within 1—4 a, a smooth desalination stage from 5—11 a, and a salinity stabilization stage from >12 a. Zong et al. (2023) concluded through the long-term drenching effect, cations and Cl^- decreased in a negative exponential power function curve, and the reduction of the sodium adsorption ratio and Cl^-/SO_4^{2-} contributed to the yearly salinity reduction in agricultural soils. The above analysis supports the results of this paper on the change of soil salinity in the irrigation district, but the literature only studies several farmlands, fails to reflect the spatial and temporal evolution of the overall salinity in the irrigation district, and fails to deeply explore the reasons for the decrease of soil salinity in drip irrigation farmland.

3.2. The main influencing factors of spatial and temporal distribution of soil salinity in oasis water-saving irrigation area

3.2.1. Screening of main influencing factors

Pearson correlation analysis was carried out on water-saving irrigation area (WSIA), irrigation area (IAR), irrigation amount (IAM), underground water diversion amount (UWDA), surface water diversion amount (SWDA), groundwater depth (GD), mineralization of groundwater (MG), annual rainfall (AR), annual water surface evaporation (AE), elevation, soil bulk density (SBD) and soil salinity (Fig. 4). Pearson

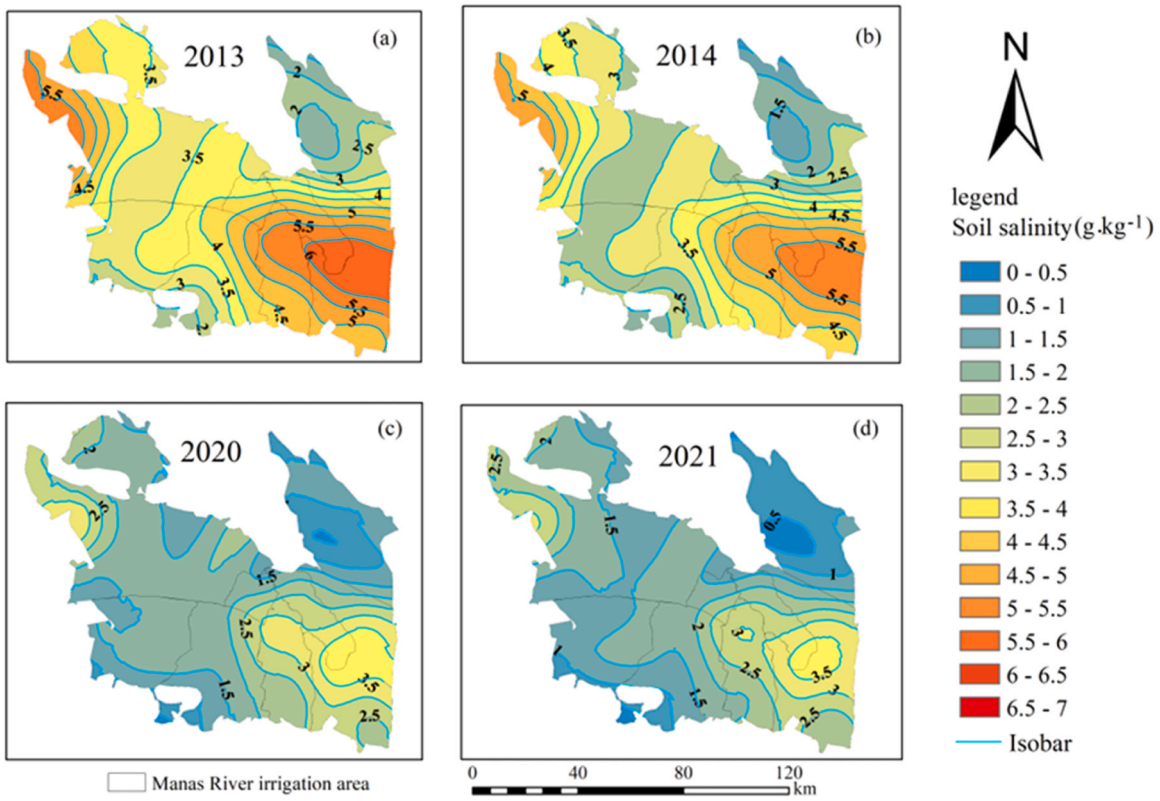

Fig. 3. Spatial distribution of average salinity in 0—100 cm soil layer in irrigation area in 2013 (a), 2014 (b), 2020 (c), and 2021 (d).

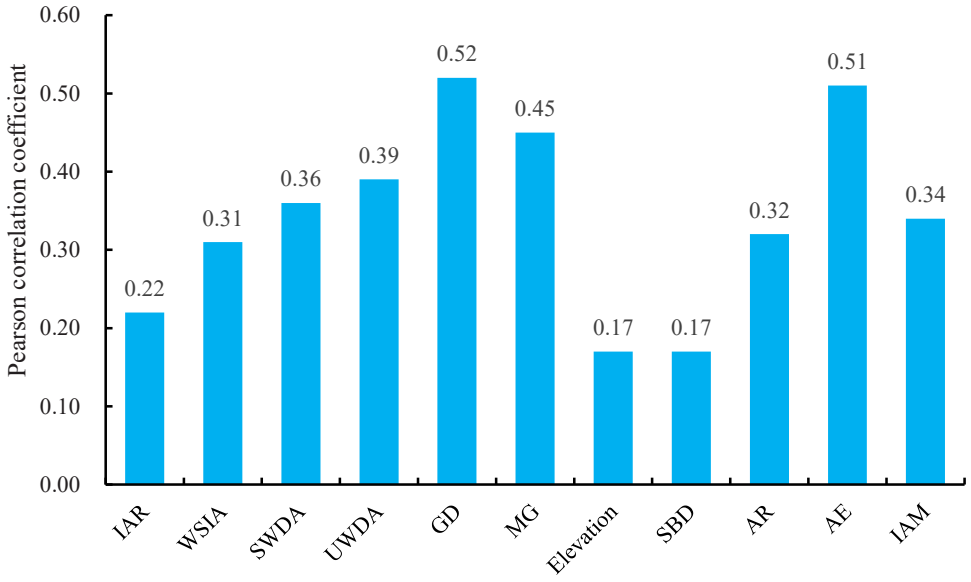

Fig. 4. Pearson correlation coefficient between influencing factors and soil salinity. (WSIA indicate: Water-saving irrigation area; UWDA indicate: Underground water diversion amount; GD indicate: Groundwater depth; MG indicate: mineralization of groundwater; AR indicate: Annual rainfall; AE indicate: Annual water surface evaporation; Elevation; SBD: Soil buck density; IAR indicate: Irrigated area; IA indicate: Irrigation amount; SWDA indicate: Surface water diversion amount.

correlation coefficient was used to evaluate the correlation between influencing factors and soil salinity. When the Pearson correlation coefficient $|r| \geq 0.8$, it is considered that the two variables are highly correlated. $0.5 \leq |r| < 0.8$, it is considered that the two variables are moderately correlated; $0.3 \leq |r| < 0.5$, the two variables can be considered low correlation. If $|r| < 0.3$, it can be considered that the two variables are irrelevant (Valenta et al., 2019). Therefore, the three factors of elevation, soil bulk density, and irrigation area, which have a low correlation with soil salinity, were removed.

To avoid the covariance that still exists in the influencing factors after the initial screening, which affects the accuracy of the constructed salt simulation model. In this paper, the variance expansion factor (VIF) test is carried out on eight factors after preliminary screening, such as water-saving irrigation area (Table 2). When VIF< 10, it means there is no multicollinearity problem (Kyriazos and Poga, 2023). The maximum VIF value is the amount of underground water diversion, which is 6.913, so there is no collinearity problem.

Characteristics of inter-annual changes in eight influencing factors include water-saving irrigation area, underground water diversion amount, surface water diversion amount, groundwater depth, groundwater mineralization of groundwater, annual rainfall, annual water surface evaporation, and irrigation amount in irrigation districts (Figs. S1–8). In 2013, 2014, 2020, and 2021, the underground and surface water diversion amounts in the irrigation district increased and decreased, with an overall increasing trend. In 2021, compared with 2013, it increased by 38.48 % and 2.21 % respectively. The water-saving irrigation area, mineralization of groundwater, and groundwater depth increased year to year by 26.30 %, 22.32 %, and 14.94 %, respectively, in 2021 compared with 2013. The annual rainfall, annual water surface evaporation, and irrigation amount showed a decreasing trend, which decreased by 2.40 %, 6.74 %, and 9.86 % in 2021 compared with 2013.

Table 2
Collinearity statistics of influencing factors.

Impact Factor	VIF
WSIA	1.287
SWDA	3.321
UWDA	6.913
GD	2.175
MG	2.013
AR	1.554
AE	1.928
IAM	4.881

3.2.2. *RF salinity modeling and analysis of the main influencing factors of spatial and temporal distribution of soil salinity in irrigation district*

The RF salt simulation model is shown in Fig. 5. The RF model's coefficient of determination (R^2) was greater than 0.66 in both the training and validation sets. The total sample's absolute error (*MAE*) was 0.35 g kg^{-1}, and the root mean square error (*RMSE*) was 0.43 g kg^{-1}. The model prediction error was small (Fu et al., 2020; Hong et al., 2020). The model can more accurately simulate the spatial and temporal changes of soil salinity in oasis water-saving irrigation areas.

The results of the SHAP interpretation algorithm based on the RF model are shown in Fig. 6. Groundwater depth, annual water surface evaporation, water-saving irrigation area, and underground water

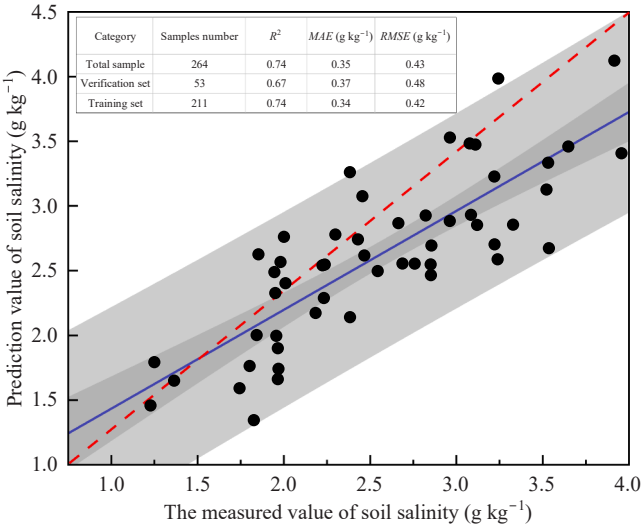

Fig. 5. Scatter plot of observed and predicted values of soil salt content validation set and training set based on RF model.

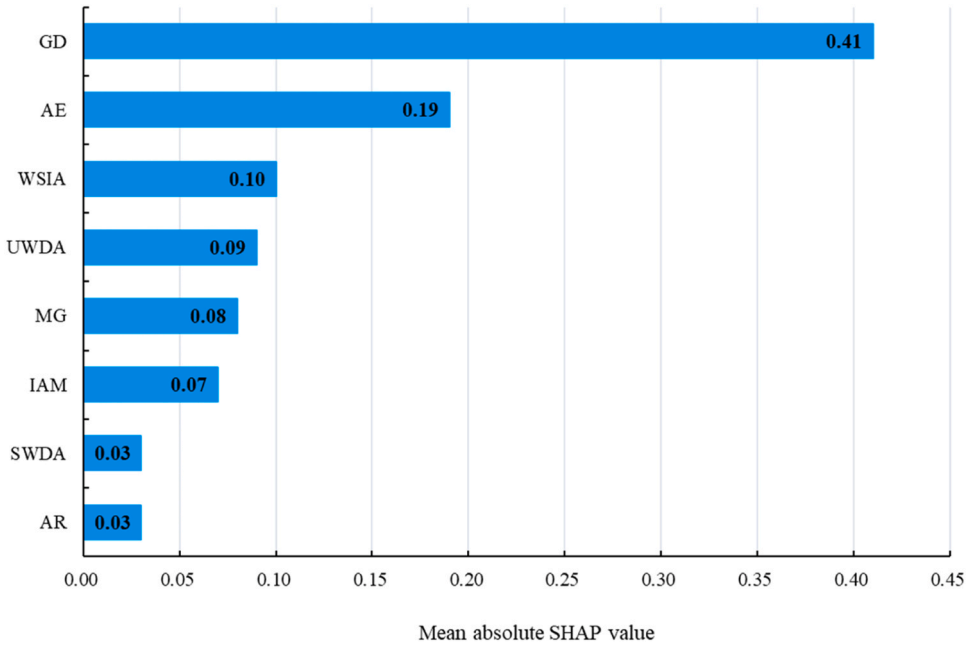

Fig. 6. The importance of influencing factors on the spatial and temporal distribution of soil salinity.

diversion amount are the most critical factors affecting the spatial and temporal distribution of soil salinity in oasis water-saving irrigation district. The SHAP values were 0.41, 0.19, 0.10, and 0.09, respectively. The rest are mineralization of groundwater, irrigation amount, surface water diversion, and annual rainfall. The ranking may reflect the relative differences in the contribution of various factors to soil salinization under different situations or conditions, but it does not mean that the lower ranking factors are not important.

Among the factors affecting soil salinity's spatial and temporal distribution, the high-value sample points of GD, WSIA, UWDA, and AR showed a negative contribution (Fig. 7). The finding explored that deeper groundwater depth, larger water-saving irrigation area, more considerable underground water diversion amount, and more annual rainfall in the oasis water-saving irrigation district can alleviate soil salt accumulation. The AE, MG, IAM, and SWDA of high-value sample points show positive contributions. The larger the AE, MG, IAM, and SWDA in the irrigation district, the more soil salinity accumulation may be promoted in the water-saving irrigation district.

Soil salinization regions worldwide have a significant common point: the groundwater depth is relatively shallow (Corre et al., 2002; Masoud et al., 2018; Pauloo et al., 2021; Zeng et al., 2021). Through investigation found the Manas River irrigation area shows high salt content distribution characteristics in the upstream and downstream regions. In the downstream of the Manas River, a natural Manas Lake is formed by overflowing springs near Xiaokai Township and Sidaohezi Township, where groundwater is relatively deep. Zhang et al. (2011) confirmed that the soil salt content was the highest near the lowest spring water overflow in the Qitai irrigation area of Xinjiang. In the upper reaches of the Manas River, there are 12 interconnected plain reservoirs, such as Daquangou and Moguhu Lake, to regulate and store water in the irrigation area. The leakage of plain reservoirs leads to a shallow groundwater depth in the region, so the soil salt content is relatively high. The finding was consistent with Wang et al. (2020) and Jan (1994) on the high soil salt content near the plain reservoir. The Manas River Irrigation District is in the arid area of northwest China, far from the ocean. It is drought, little rain, and intense evaporation all the year round. That quickly causes soil salt to accumulate on the surface, showing the phenomenon of 'surface accumulation' (Wichelns and Qadir, 2015).

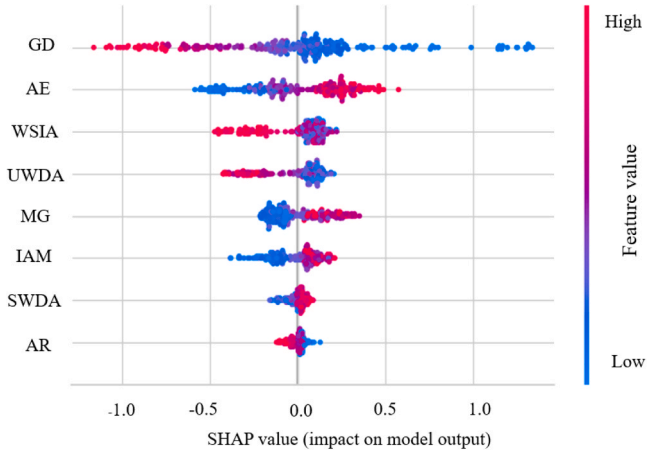

Fig. 7. SHAP summary map of influencing factors of spatial and temporal distribution of soil salinity.

The evolution of soil salinity results from the interaction of many natural and human factors (Zhou et al., 2010; Tian et al., 2019). On a small scale, it is more disturbed by human factors; on a large scale, it is more affected by natural factors such as groundwater, topography, and climatic conditions (Zhang et al., 2014a). Based on a large number of measured data, this study used an interpretable machine learning model to obtain the order of importance of the influencing factors of soil salinity temporal and spatial evolution in oasis irrigation district: GD> AE> WSIA> UWDA> MG >IAM> SWDA> AR. This is similar to the results of groundwater, climate and artificial irrigation affecting the evolution of soil salinity (Panagopoulos et al., 2006; Dai et al., 2011; Zhang et al., 2014b; Nachshon, 2018). However, this study quantified the contribution of each influencing factor on top of that using the SHAP algorithm.

3.3. Technical measures to alleviate the possible secondary salinization in an oasis water-saving irrigation district

3.3.1. Groundwater depth control measures

The SHAP characteristic dependence diagram (PDP diagram) shows the response of SHAP value to the change of main influencing factors, the influence threshold of influencing factors on the spatial and

temporal distribution of soil salinity, and the influence of interaction between influencing factors on SHAP value (Fig. 8). The influence of groundwater depth on soil salt content showed a nonlinear decline-steady trend. Groundwater depth <4.0 m showed a positive contribution, and the effect of rising groundwater depth on soil salinity aggregation was significant. The threshold range of groundwater depth affecting the spatial and temporal distribution of soil salinity in an oasis water-saving irrigation district is about 4.0—6.0 m. When the groundwater depth is greater than 6 m and increases, the SHAP value of soil salt content tends to be gentle, showing a negative contribution. Under the interaction of groundwater depth and irrigation amount, the sample points affected by lower irrigation amount significantly positively contributed to soil salt content.

In previous studies, the methods for determining critical groundwater depth in irrigation districts can be summarized as statistical analysis methods based on field measurement data, theoretical model calculation methods, and indirect methods based on remote sensing data. Qi et al. (2012) established the correlation between oasis ecological vegetation growth and groundwater depth through measured data and analyzed and determined that the threshold of groundwater depth in arid areas is 3.5—4.0 m. Abliz et al. (2016) used FEFLOW to simulate the change of groundwater burial depth in different periods, and combined it with the spatial distribution law of vegetation to obtain that soil salinity increased significantly with the decrease of groundwater burial depth when the groundwater burial depth was <4.0 m in Xinjiang Keria Oasis. Qi et al. (2021) established a correlation between soil salinity and groundwater depth obtained by remote sensing and obtained that the buried depth of 4.8—6.1 m is the threshold value of groundwater level in Qian'an County, Hebei Province. This is similar to the results of this study, which used the SHAP algorithm to interpret the predictions of the RF salinity simulation model to identify a range of water table thresholds of approximately 4.0—6.0 m in water-saving irrigation district.

3.3.2. *Irrigation amount control measures*

Irrigation amount affects the spatial and temporal distribution of soil salinity in an oasis water-saving irrigation district at a threshold of about 5500—6000 m^3 ha^{-1}. When the irrigation amount was <5500 m^3 ha^{-1}, there was a positive contribution to soil salinity in agricultural fields, and the positive contribution decreased with increasing irrigation amount. The positive contribution of sample points affected by high groundwater salinity is significant.

According to the summary data of the annual irrigation report of Shihezi City, Shawan City, and Manas County, the irrigated area of Manas River Irrigation District in 2021 was 3.41 × 10^6 ha, of which cotton accounted for 87.07 %, wheat accounted for 5.74 %, and the others were crops such as maize, grapes, and processed tomatoes. Since the application of drip irrigation under mulch technology was attempted in the Manas River Irrigation District in 1996, a large number of scholars have carried out research on the irrigation system of drip-irrigated cotton and wheat in the northern border through irrigation tests and water balance calculations. It was determined that the irrigation amount during the cotton growth period was about 4200—4500 m^3 ha^{-1} (Gao et al., 2019), and the irrigation amount during the wheat growth period was about 4050—4120 m^3 ha^{-1} (Mekonnen, 2017). The above results have played a positive role in guiding agricultural production in oasis areas. However, the long-term application of irrigation amount determined only from the perspective of crop physiological water demand in arid oasis areas may cause soil secondary salinization. Therefore, scholars have researched stubble or winter irrigation and determined the non-fertile period salt washing and entropy lifting amount of 900—1200 m^3 ha^{-1}. The sum of the irrigation, as mentioned earlier, amount of cotton and wheat in the growth period and the non-growth period of salt washing and entropy extraction is similar to the results of the suitable irrigation amount of the Manas River Irrigation District, which is 5500—6000 m^3 ha^{-1} considering the secondary contribution to soil salinity in this study. As for how much surface water and groundwater are respectively, and how much surface water and groundwater salinity will not cause secondary soil salinization, further research is needed.

4. Conclusions

The soil salinity in the water-saving irrigation district of the oasis was moderately variable in different years and soil layers (C_v = 46.74 %—51.80 %). The salt content in the horizontal direction is higher in the upstream and downstream areas of the irrigation district, while the variability in the vertical direction gradually decreases with increasing depth. The random forest model can accurately simulate soil salinity's temporal and spatial changes in an oasis irrigation district. The importance of the factors affecting the spatial and temporal evolution of soil salinity in the irrigation district are ranked as groundwater depth, annual water surface evaporation, water-saving irrigation area, underground water diversion amount, groundwater mineralization, irrigation amount, surface water diversion amount, and annual rainfall. Positive contribution to soil salinity accumulation in water-saving irrigation districts at groundwater depths <4.0 m. Under the interaction of groundwater depth and irrigation amount, the positive contribution of lower irrigation amount to soil salinity content was significant. When the irrigation amount was <5500 m^3 ha^{-1}, there was a positive contribution of soil salinity accumulation in the irrigation district. Under the interaction of irrigation amount and mineralization of groundwater, the higher mineralization of groundwater has a significant positive contribution to soil salt content. The suitable groundwater depth is 4.0—6.0 m and the suitable irrigation amount is 5500—6000 m^3 ha^{-1} in the water-

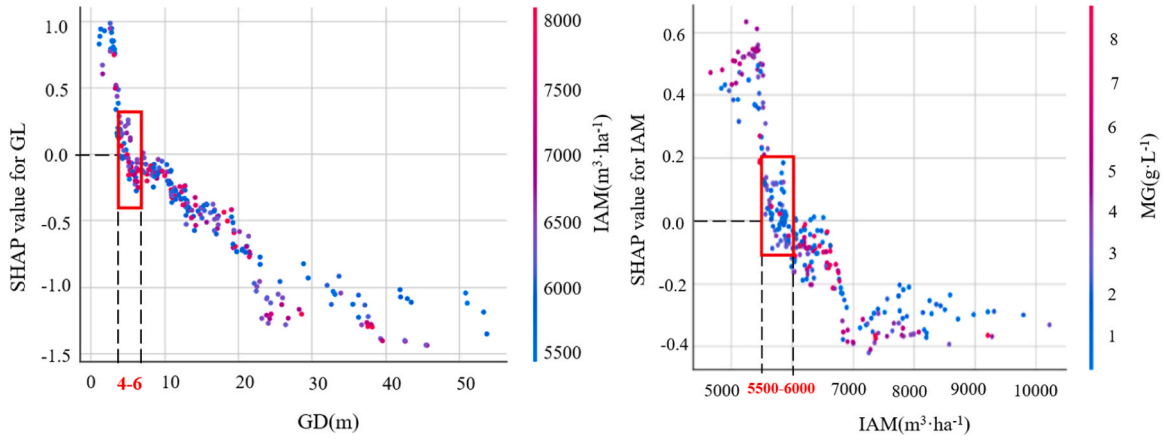

Fig. 8. The main influencing factors of spatial and temporal distribution of soil salinity.

saving irrigation district dominated by cotton and wheat. In conclusion, groundwater depth and annual water surface evaporation are the most critical influences on the spatial and temporal variability of soil salinity in the inland arid zone of Northwest China. Therefore, although soil salinity in the water-saving irrigation district represented by the Manas River Irrigation District gradually decreases with time, the prevention and management of soil salinization in the Northwest Oasis can still not be ignored due to the intense evaporation in the arid zone. However, production through scientific groundwater depth control, reasonable irrigation systems, and other regulatory measures can alleviate water-saving irrigation districts' secondary salinization problems and achieve sustainable development.

CRediT authorship contribution statement

Taisheng Du: Writing – review & editing, Supervision, Resources, Project administration. **Risheng Ding:** Writing – review & editing, Resources, Formal analysis. **Wenhao Li:** Writing – original draft, Methodology, Investigation, Data curation. **Shaozhong Kang:** Writing – review & editing, Supervision, Resources, Project administration. **Minzhong Zou:** Writing – review & editing, Resources, Formal analysis.

Declaration of Competing Interest

The authors declare that we have no known competing financial interests or personal relationships that could have appeared to influence the work reported in this paper

Data Availability

Data will be made available on request.

Acknowledgments

This work was supported by the National Natural Science Foundation of China 'Study on Water and Salt Simulation and Multidimensional Critical Regulation Mechanism in Typical Arid Oasis Irrigation Area (52209064)' and the National Natural Science Foundation of China 'Study on the Mechanism of the Effect of Three Water Transformation on Soil Salt Migration in Cotton Field with Long-term Drip Irrigation in Arid Area (52279040)'.

Appendix A. Supporting information

Supplementary data associated with this article can be found in the online version at doi:10.1016/j.agwat.2024.109007.

References

Abliz, A., Tiyip, T., Ghulam, A., Halik, Ü., Ding, J.-l, Sawut, M., Zhang, F., Nurmemet, I., Abliz, A., 2016. Effects of shallow groundwater table and salinity on soil salt dynamics in the Keriya Oasis, Northwestern China. Environ. Earth Sci. 75, 1–15. https://doi.org/10.1007/s12665-015-4794-8.

Bouksila, F., Bahri, A., Berndtsson, R., Persson, M., Rozema, J., Van der Zee, S.E., 2013. Assessment of soil salinization risks under irrigation with brackish water in semiarid Tunisia. Environ. Exp. Bot. 92, 176–185. https://doi.org/10.1016/j.envexpbot.2012.06.002.

Corre, M.D., Schnabel, R.R., Stout, W.L., 2002. Spatial and seasonal variation of gross nitrogen transformations and microbial biomass in a Northeastern US grassland. Soil Biol. Biochem. 34, 445–457. https://doi.org/10.1016/S0038-0717(01)00198-5.

Corwin, D.L., 2021. Climate change impacts on soil salinity in agricultural areas. Eur. J. Soil Sci. 72, 842–862. https://doi.org/10.1111/ejss.13010.

Dai, X., Huo, Z., Wang, H., 2011. Simulation for response of crop yield to soil moisture and salinity with artificial neural network. Field Crops Res. 121, 441–449. https://doi.org/10.1016/j.fcr.2011.01.016.

Danierhan, S., Shalamu, A., Tumaerbai, H., Guan, D., 2013. Effects of emitter discharge rates on soil salinity distribution and cotton (*Gossypium hirsutum L.*) yield under drip irrigation with plastic mulch in an arid region of Northwest China. J. Arid Land 5, 51–59. https://doi.org/10.1007/s40333-013-0141-7.

Deng, X.-P., Shan, L., Zhang, H., Turner, N.C., 2006. Improving agricultural water use efficiency in arid and semiarid areas of China. Agric. Water Manag. 80, 23–40. https://doi.org/10.1016/j.agwat.2005.07.021.

Feng, Z., Wang, L., Peng, Q., Li, J., Liang, T., 2022. Effect of environmental factors on soil properties under different land use types in a typical basin of the North China Plain. J. Clean. Prod. 344, 131084 https://doi.org/10.1016/j.jclepro.2022.131084.

Fu, Z., Jiang, J., Gao, Y., Krienke, B., Wang, M., Zhong, K., Cao, Q., Tian, Y., Zhu, Y., Cao, W., 2020. Wheat growth monitoring and yield estimation based on multi-rotor unmanned aerial vehicle. Remote Sens. 12, 508. https://doi.org/10.3390/rs12030508.

Gao, H., Ma, H., Khan, A., Xia, J., Hao, X., Wang, F., Luo, H., 2019. Moderate drip irrigation level with low mepiquat chloride application increases cotton lint yield by improving leaf photosynthetic rate and reproductive organ biomass accumulation in arid region. Agronomy 9, 834. https://doi.org/10.3390/agronomy9120834.

Haj-Amor, Z., Araya, T., Kim, D.-G., Bouri, S., Lee, J., Ghiloufi, W., Yang, Y., Kang, H., Jhariya, M.K., Banerjee, A., 2022. Soil salinity and its associated effects on soil microorganisms, greenhouse gas emissions, crop yield, biodiversity and desertification: a review. Sci. Total Environ. 843, 156946 https://doi.org/10.1016/j.scitotenv.2022.156946.

Hammad, H.M., Abbas, F., Ahmad, A., Farhad, W., Wilkerson, C.J., Hoogenboom, G., 2023. Water and nitrogen management influence on oil and protein concentration in maize. Agron. J. 115, 557–568. https://doi.org/10.1002/agj2.21275.

Hong, Y., Guo, L., Chen, S., Linderman, M., Mouazen, A.M., Yu, L., Chen, Y., Liu, Y., Liu, Y., Cheng, H., 2020. Exploring the potential of airborne hyperspectral image for estimating topsoil organic carbon: effects of fractional-order derivative and optimal band combination algorithm. Geoderma 365, 114228. https://doi.org/10.1016/j.geoderma.2020.114228.

Hopmans, J.W., Qureshi, A., Kisekka, I., Munns, R., Grattan, S., Rengasamy, P., Ben-Gal, A., Assouline, S., Javaux, M., Minhas, P., 2021. Critical knowledge gaps and research priorities in global soil salinity. Adv. Agron. 169, 1–191. https://doi.org/10.1016/bs.agron.2021.03.001.

Hou, X., Xiang, Y., Fan, J., Zhang, F., Hu, W., Yan, F., Xiao, C., Li, Y., Cheng, H., Li, Z., 2022. Spatial distribution and variability of soil salinity in film-mulched cotton fields under various drip irrigation regimes in southern Xinjiang of China. Soil Res. 223, 105470 https://doi.org/10.1016/j.still.2022.105470.

Jan, vS., 1994. Irrigation—a blessing or a curse. Agric. Water Manag. 25, 203–219. https://doi.org/10.1016/0378-3774(94)90061-2.

John, K., Bouslihim, Y., Bouasria, A., Razouk, R., Hssaini, L., Isong, I.A., Ait M'barek, S., Ayito, E.O., Ambrose-Igho, G., 2022. Assessing the impact of sampling strategy in random forest-based predicting of soil nutrients: a study case from northern Morocco. GeoIn 37, 11209–11222. https://doi.org/10.1080/10106049.2022.2048091.

Karimzadeh, S., Hartman, S., Chiarelli, D.D., Rulli, M.C., D'Odorico, P., 2024. The tradeoff between water savings and salinization prevention in dryland irrigation. Adv. Water Resour. 183, 104604 https://doi.org/10.1016/j.advwatres.2023.104604.

Kyriazos, T., Poga, M., 2023. Dealing with multicollinearity in factor analysis: the problem, detections, and solutions. Open J. Stat. 13, 404–424. https://doi.org/10.4236/ojs.2023.133020.

Li, X., Li, Y., Wang, B., Sun, Y., Cui, G., Liang, Z., 2022. Analysis of spatial-temporal variation of the saline-sodic soil in the west of Jilin Province from 1989 to 2019 and influencing factors. Catena 217, 106492. https://doi.org/10.1016/j.catena.2022.106492.

Li, S., Tang, Q., Lei, J., Xu, X., Jiang, J., Wang, Y., 2015. An overview of non-conventional water resource utilization technologies for biological sand control in Xinjiang, northwest China. J. Environ. Earth Sci. 73, 873–885. https://doi.org/10.1007/s12665-014-3443-y.

Li, D., Zhao, Y., Li, M., Zhou, X., Li, W., Jia, Y., 2023. Water and salt replacement through soil salt leaching under brackish water conditions with subsurface pipe drainage. Irrig. Drain. 72, 807–822. https://doi.org/10.1002/ird.2803.

Masoud, A.A., El-Horiny, M.M., Atwia, M.G., Gemail, K.S., Koike, K., 2018. Assessment of groundwater and soil quality degradation using multivariate and geostatistical analyses, Dakhla Oasis, Egypt. JAFES 142, 64–81. https://doi.org/10.1016/j.jafrearsci.2018.03.009.

Mekonnen, A., 2017. Effects of seeding rate and row spacing on yield and yield components of bread wheat (*Triticum aestivum L.*) in Gozamin District, East Gojam Zone, Ethiopia. J. Biol., Agric. Healthc. 7, 19–37.

Meng, Y., Yang, N., Qian, Z., Zhang, G., 2020. What makes an online review more helpful: an interpretation framework using XGBoost and SHAP values. J. Theor. Appl. Electron. Commer. Res. 16, 466–490. https://doi.org/10.3390/jtaer16030029.

Mut, R., Şeker, C., Negiş, H., 2022. Effectiveness of conventional and minimized tillage practices on soil quality properties and maize yield attributes. Selcuk. J. Agric. Food Sci. 36 (3), 438–446. https://doi.org/10.15316/sjafs.2022.058.

Nachshon, U., 2018. Cropland soil salinization and associated hydrology: trends, processes and examples. Water 10, 1030. https://doi.org/10.3390/w10081030.

Panagopoulos, T., Jesus, J., Antunes, M., Beltrão, J., 2006. Analysis of spatial interpolation for optimising management of a salinized field cultivated with lettuce. Eur. J. Agron. 24, 1–10. https://doi.org/10.1016/j.eja.2005.03.001.

Pauloo, R.A., Fogg, G.E., Guo, Z., Harter, T., 2021. Anthropogenic basin closure and groundwater salinization (ABCSAL). J. Hydrol. 593, 125787 https://doi.org/10.1016/j.jhydrol.2020.125787.

Qi, F., JiaZhong, P., JianGuo, L., HaiYang, X., JianHua, S., 2012. Using the concept of ecological groundwater level to evaluate shallow groundwater resources in hyperarid desert regions. J. Arid Land 4, 378–389. https://doi.org/10.3724/SP.J.1227.2012.00378.

Qi, Z., Xiao, C., Wang, G., Liang, X., 2021. Study on ecological threshold of groundwater in typical salinization area of Qian'an County. Water 13, 856. https://doi.org/10.3390/w13060856.

Ren, D., Wei, B., Xu, X., Engel, B., Li, G., Huang, Q., Xiong, Y., Huang, G., 2019. Analyzing spatiotemporal characteristics of soil salinity in arid irrigated agro-ecosystems using integrated approaches. Geoderma 356, 113935. https://doi.org/10.1016/j.geoderma.2019.113935.

Rosemary, F., Indraratne, S., Weerasooriya, R., Mishra, U., 2017. Exploring the spatial variability of soil properties in an Alfisol soil catena. Catena 150, 53–61. https://doi.org/10.1016/j.catena.2016.10.017.

Salcedo, F.P., Cutillas, P.P., Cabañero, J.J.A., Vivaldi, A.G., 2022. Use of remote sensing to evaluate the effects of environmental factors on soil salinity in a semi-arid area. Sci. Total Environ. 815, 152524 https://doi.org/10.1016/j.scitotenv.2021.152524.

Scudiero, E., Skaggs, T., Corwin, D., 2014. Regional scale soil salinity evaluation using Landsat 7, western San Joaquin Valley, California, USA. Geoderma 2-3, 82–90. https://doi.org/10.1016/j.geodrs.2014.10.004.

Shen, Y., Li, S., Chen, Y., Qi, Y., Zhang, S., 2013. Estimation of regional irrigation water requirement and water supply risk in the arid region of Northwestern China 1989-2010. Agric. Water Manag. 128, 55–64. https://doi.org/10.1016/j.agwat.2013.06.014.

Sun, G., Zhu, Y., Ye, M., Yang, Y., Yang, J., Mao, W., Wu, J., 2022. Regional soil salinity spatiotemporal dynamics and improved temporal stability analysis in arid agricultural areas. J. Soils Sediment. 22, 272–279. https://doi.org/10.1007/s11368-021-03074-y.

Taghizadeh-Mehrjardi, R., Minasny, B., Sarmadian, F., Malone, B., 2014. Digital mapping of soil salinity in Ardakan region, central Iran. Geoderma 213, 15–28. https://doi.org/10.1016/j.geoderma.2013.07.020.

Tian, A., Fu, C., Su, X.-Y., Yau, H.-T., Xiong, H., 2019. Classifying and predicting salinization level in arid area soil using a combination of Chua's circuit and fractional order sprott chaotic system. Sensors 19, 4517. https://doi.org/10.3390/s19204517.

Valenta, R.K., Kemp, D., Owen, J.R., Corder, G.D., Lèbre, É., 2019. Re-thinking complex orebodies: consequences for the future world supply of copper. J. Clean. Prod. 220, 816–826. https://doi.org/10.1016/j.jclepro.2019.02.146.

Wang, J., Ding, J., Yu, D., Ma, X., Zhang, Z., Ge, X., Teng, D., Li, X., Liang, J., Lizaga, I., 2019a. Capability of Sentinel-2 MSI data for monitoring and mapping of soil salinity in dry and wet seasons in the Ebinur Lake region, Xinjiang, China. Geoderma 353, 172–187. https://doi.org/10.1016/j.geoderma.2019.06.040.

Wang, Z., Fan, B., Guo, L., 2019b. Soil salinization after long-term mulched drip irrigation poses a potential risk to agricultural sustainability. Eur. J. Soil Sci. 70, 20–24. https://doi.org/10.1111/ejss.12742.

Wang, J., Liu, Y., Wang, S., Liu, H., Fu, G., Xiong, Y., 2020. Spatial distribution of soil salinity and potential implications for soil management in the Manas River watershed, China. Soil Use Manag. 36, 93–103. https://doi.org/10.1111/sum.12539.

Wei, Y., Shi, Z., Biswas, A., Yang, S., Ding, J., Wang, F., 2020. Updated information on soil salinity in a typical oasis agroecosystem and desert-oasis ecotone: Case study conducted along the Tarim River, China. Sci. Total Environ. 716, 135387 https://doi.org/10.1016/j.scitotenv.2019.135387.

Wichelns, D., Qadir, M., 2015. Achieving sustainable irrigation requires effective management of salts, soil salinity, and shallow groundwater. Agric. Water Manag. 157, 31–38. https://doi.org/10.1016/j.agwat.2014.08.016.

Xie, W., Yang, J., Yao, R., Wang, X., 2021. Spatial and temporal variability of soil salinity in the Yangtze River estuary using electromagnetic induction. Remote Sens. 13, 1875. https://doi.org/10.3390/rs13101875.

Yao, R., Yang, J., 2010. Quantitative evaluation of soil salinity and its spatial distribution using electromagnetic induction method. Agric. Water Manag. 97, 1961–1970. https://doi.org/10.1016/j.agwat.2010.02.001.

Zeng, Y., Zhou, J., Zhou, Y., Sun, Y., Zhang, J., 2021. Causes of groundwater salinization in the plain area of Kashgar River Basin in Xinjiang, China. Environ. Earth Sci. 80, 801. https://doi.org/10.1007/s12665-021-10086-x.

Zhang, Z., Jilili, Abuduwaili, Hamid, Y., 2014b. The occurrence, sources and spatial characteristics of soil salt and assessment of soil salinization risk in Yanqi Basin, Northwest China. PLoS One 9, e106079. https://doi.org/10.1371/journal.pone.0106079.

Zhang, W.-T., Wu, H.-Q., Gu, H.-B., Feng, G.-L., Wang, Z., Sheng, J.-D., 2014a. Variability of soil salinity at multiple spatio-temporal scales and the related driving factors in the oasis areas of Xinjiang, China. Pedosphere 24, 753–762. https://doi.org/10.1016/S1002-0160(14)60062-X.

Zhang, F., Xiong, H., Tian, Y., Luan, F., 2011. Impacts of regional topographic factors on spatial distribution of soil salinization in Qitai Oasis. Res. Environ. Sci. 24, 731–739.

Zhao, Y., Shi, H., Miao, Q., Yang, S., Hu, Z., Hou, C., Yu, C., Yan, Y., 2023. Analysis of spatial and temporal variability and coupling relationship of soil water and salt in cultivated and wasteland at branch canal scale in the Hetao irrigation district. Agronomy 13, 2367. https://doi.org/10.3390/agronomy13092367.

Zhou, H., Chen, Y., Li, W., 2010. Soil properties and their spatial pattern in an oasis on the lower reaches of the Tarim River, northwest China. Agric. Water Manag. 97, 1915–1922. https://doi.org/10.1016/j.agwat.2010.07.004.

Zong, R., Wang, Z., Li, W., Li, H., Ayantobo, O.O., 2023. Effects of practicing long-term mulched drip irrigation on soil quality in Northwest China. Sci. Total Environ. 878, 163247 https://doi.org/10.1016/j.scitotenv.2023.16324.